A METHOD FOR THE CHARACTERISATION OF SPATIAL STRUCTURES OBSERVED IN CEREBRAL FMRI DATA

Camille Gómez-Laberge[12], Andy Adler[1], Matthew J. Hogan[2]
[1]*Systems & Computer Engineering, Carleton University*
[2]*Neuroscience, Ottawa Health Research Institute*

I. INTRODUCTION

Functional Magnetic Resonance Imaging (fMRI) can detect venous concentration changes of deoxygenated hemoglobin. Cerebral blood flow is locally regulated by pre-capillary arteriolar smooth muscles [1]. Consequently, fMRI images inherit the spatial characteristic of localised signal change. In addition, spurious voxels also exhibit significant fluctuations due to instrumental and physiological noise. The superposition of these effects emerge when analysing the images for significant temporal changes.

Hence, a characterisation of the spatial structures observed in the data may provide relevant information about the images and also assist in noise reduction. In order to model the spatial characteristics observed in these images, a quantitative measure of the *contiguity* of the voxel maps obtained from analysis is useful.

In this study, a novel method for image analysis is developed based on a quantitative definition of contiguity. A synthesis of fMRI voxel maps, typically observed in clustering techniques, is developed using Gaussian random fields (GRF). A performance figure-of-merit is obtained by comparison with the Euler number of level-sets from the image. Contiguity characterisations are obtained in relation to GRF covariance and signal-to-noise ratio. Finally, a demonstration of the method on 3D fMRI data obtained from an event-related paradigm is presented.

II. METHODS

This methodology applies to gray scale images discretised into voxels. The typical images to be analysed are rather sparse, where few non-zero voxels exist representing a signal that is temporally correlated to a target function. The gray scale value of the voxels is the correlation coefficient between these signals. The synthesis model is developed in 2D for illustrative purposes; however, it is easily extendible to 3D for practical applications as is shown in section III.

A quantitative definition of contiguity

Some terminology is first needed to define contiguity. Two voxels sharing a face are called *adjacent*. A sequence of adjacent voxels is defined as a *group*. Let L be the number of non-zero voxels in an image, which can then be written as the series

$$L = 1g_1 + 2g_2 + \cdots + Mg_M, \quad (1)$$

where g_l is the number of groups containing l voxels, and M is the largest group in the image. We define a group to be *contiguous* if it contains at least m voxels. Thus, by setting $g_l=0$ for $l<m$, we obtain the fraction of voxels belonging to contiguous groups

$$0 \le \frac{1}{L}\sum_{l=m}^{M} lg_l \le 1. \quad (2)$$

To distinguish an image containing many groups from one containing fewer groups, we impose a penalty on the total number of contiguous groups G. From this, we define the contiguity c of an image as the series

$$c = \frac{1}{GL}\sum_{l=m}^{M} lg_l. \quad (3)$$

Notice that the reciprocal of c provides an estimate of the total number of contiguous groups in the image. Figure 1 illustrates the contiguity of binary images progessively decreasing in contiguity.

A synthesis model of fMRI voxel map images

This section develops a model based on the empirical examination of voxel maps obtained during an fMRI event-related motor-task design on two normal subjects.

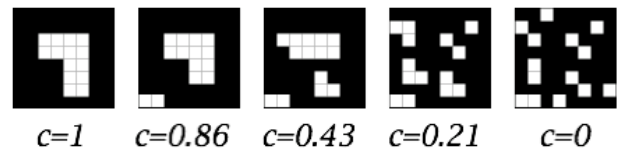$c=1$ $c=0.86$ $c=0.43$ $c=0.21$ $c=0$

Figure 1: The contiguity of five example images, each having $L=14$. The smallest contiguous group size is defined as $m=3$.

The voxel maps were obtained from a *c*-means cluster analysis as described in [2]. Each map contains a subset of voxels whose temporal signals are positively correlated to a target function (the cluster centroid). The voxels with large coefficients tend to be localised, where as the others with low correlations are rather sporadic. Our model synthesises images where the prominence of these characteristics are controlled by two parameters: the spatial covariance, and signal-to-noise ratio (SNR).

The model uses a superposition of signal and noise components, each defined as a GRF sampled on a rectangular lattice [3,4]. Consider their respective uncorrelated Gaussian processes, independent of one another

$$\mathbf{Y}[\mathbf{x}] \sim N(\mu_Y, \sigma_Y^2),$$

$$\mathbf{N}[\mathbf{x}] \sim N(\mu_N, \sigma_N^2). \tag{4}$$

Now, we introduce spatial correlation in the signal source with a *d*-dimensional Gaussian kernel

$$k[\mathbf{x}] = \frac{1}{(2\pi)^{d/2} |\mathbf{\Sigma}_k|^{1/2}} \exp\left\{-\frac{1}{2}\mathbf{x}^{\mathrm{T}}\mathbf{\Sigma}_k^{-1}\mathbf{x}\right\}, \tag{5}$$

such that the convolved signal $\mathbf{S}=k*\mathbf{Y}$ is spatially correlated according to the covariance matrix $\mathbf{\Sigma}_k$.

We define the superposition of these random fields as our model

$$\mathbf{R} = \max\{\mathbf{S}, \mathbf{N}\}. \tag{6}$$

In our contiguity analysis in section III, we implement $\mathbf{R}$ for $d=2$ on a 64×64 8-bit pixel lattice with parameters σ^2 such that $\mathbf{\Sigma}_k=\sigma^2\mathbf{I}_d$, and $SNR= s_S^2 / \sigma_N^2$. We use the sample variance for each realisation of $\mathbf{S}$. The top row of figure 2 shows some typical realisations of $\mathbf{R}(\sigma^2, SNR)$ obtained when varying the parameter σ^2 at $SNR=1.5$.

Contiguity performance figure-of-merit

The contiguity defined in (3) is applied to the level-set images obtained from realisations of $\mathbf{R}$. A level-set is a binary image where all pixels above an intensity threshold are set to one and otherwise zero [3]. The contiguity of these level-sets is compared to the classic Euler number ψ, which counts the number of groups minus the number of holes in an image. To obtain comparable results for the Euler number, we erode spurious pixels. The performance figure-of-merit used to test the contiguity is the root-mean-square (RMS) difference of the group-count obtained by both methods over 100 realisations.
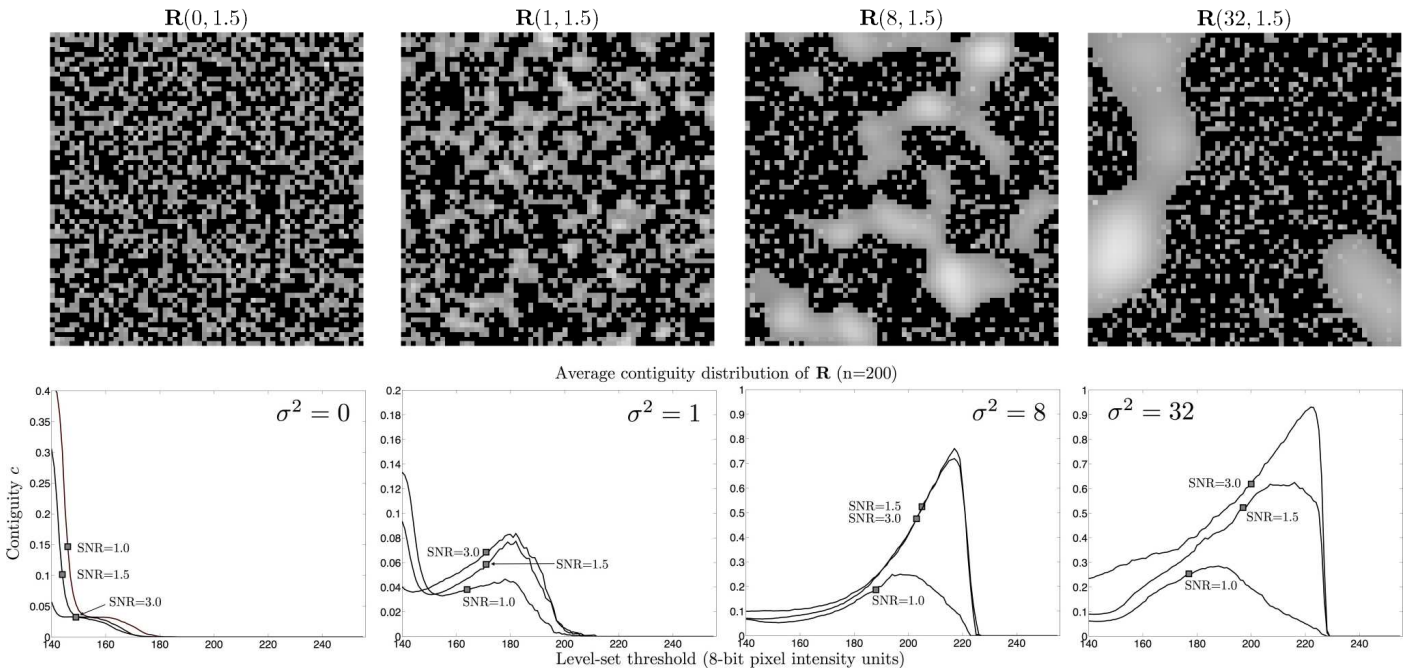

Figure 2: Synthesis of fMRI voxel maps using a Gaussian random field model. (*Top row*) Four typical 2D realisations of the model $\mathbf{R}(\sigma^2, SNR)$ on a 64x64 8-bit pixel lattice. (*Bottom row*) Corresponding contiguity distribution averaged over 200 realisations for all combinations of parameters σ^2=0, 1, 8, 32; SNR=1.0, 1.5, 3.0.

III. RESULTS

Synthetic data

We selected a subset of parameter values for the synthesis model that were representative of the range of fMRI voxel maps previously observed. For each pair of parameter values, we generated 200 realisations of our model $\mathbf{R}(\sigma^2, SNR)$. For each realisation, we computed the contiguity values on the binary level-sets with threshold starting from 255 down to 0. The resulting "contiguity distributions" are a plot of these contiguity values versus the level-set threshold. The bottom row of figure 2 shows the averaged (n=200) contiguity distributions for parameters σ^2=0, 1, 8, 32 shown in the graphs from left to right, respectively (error bars were unnoticeable at this scale). Also shown on these graphs are the median values (marked as squares) for each distribution. The distributions flatten for thresholds below 140 and are not shown, since our model rejects all pixels below this value (as was described in section II).

The graphs in figure 2 reveal a rapid growth in area of the contiguity distribution as σ^2 increases, as well as an incremental growth in each graph as SNR increases. These trends are also reflected in the median values shown. An apparent contradiction is visible here: the first graph shows a lower median value for higher SNR. Indeed a low SNR value will blend the uncorrelated signal uniformly with the noise signal. Thus, any level-set admits or rejects both signal and noise components. This explains why the distribution vanishes beyond threshold 180 and grows rapidly for lower values, producing a single entangled chain-like group. Another interesting case is the

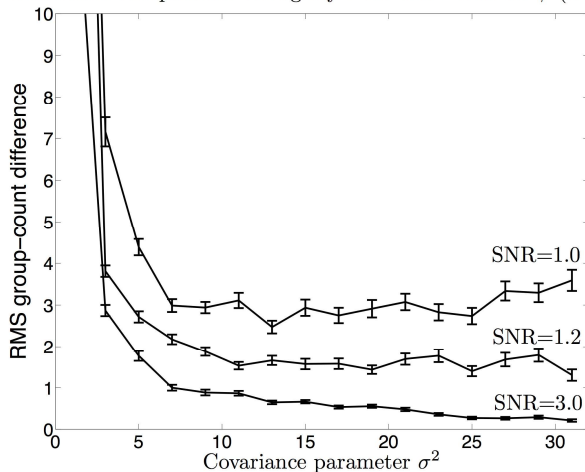Performance comparison: contiguity c vs. Euler number ψ ($n = 200$)

Figure 3: Performance comparison of the contiguity method with the Euler number method.

insensitivity of a SNR increase between 1.5 and 3.0 for σ^2=8. Here the median values are slightly reversed; however, the contiguity distribution remains larger for the higher SNR.

To ascertain the performance of the proposed method, we computed the contiguity median for 100 realisations of $\mathbf{R}(\sigma^2, SNR)$ for all integer values σ^2 with SNR=1.0, 1.2, and 3.0. These values were compared with Euler number to obtain the figure-of-merit described in section II. The mean and standard error values of the RMS group-count difference between methods are graphed in figure 3. A uniform reduction in the count difference between methods is seen as SNR increases. Secondly, for the curves corresponding to SNR 1.2 and 3.0, a gradual reduction in count difference occurs as σ^2 increases. Moreover, the graph reveals large differences between methods for σ^2<5. This is expected since these parameter values produce noisy images of spurious signal and noise components similar to those shown on the left side of figure 2. As described in section II, the Euler number method erodes spurious pixels, leaving an almost blank image, whereas the contiguity measure attempts to disentangle both components, and leaves both noise and signal combined.

fMRI data

An excerpt of the results from an analysis of fMRI blood-oxygen level dependent (BOLD) data acquired during a visually cued motor-task on one normal subject is presented in figure 4. The spatial contiguity method was paired with a temporal cross-correlation method as cluster *selection criteria* for data-driven fMRI analysis [5]. Briefly, these data were first clustered using a correlation measure between all voxel time sequences. Figure 4 shows two selected cluster voxel maps (one per row). Each voxel map is shown along with the anatomical outline in superior transcranial, right sagittal, and posterior coronal views, from left to right, respectively. Their centroid fMRI BOLD response is graphed (solid line) versus time in 2 second intervals along with the paradigm sequence (dashed line). The right most graph is the contiguity distribution plotted versus the PPMC coefficient between each voxel and the centroid time sequences. The squares mark the median value: the level-sets used to display the voxel maps.

Although both voxel maps exhibit significant temporal cross-correlation with the paradigm, as well as large contiguity values, the top row voxel map appears more correlated and localised than the bottom one. The contiguity distribution shows that its member voxels with PPMC > 0.8 are perfectly contiguous,

localised in the expected cerebellar lobe, contralateral to the cerebral sensorimotor cortex that was also identified in [5]. The bottom row voxel map, although significant, is suspected of containing a venous artefact emerging bilaterally from the transverse sinus. Its contiguity distribution characterises the map as consisting of several groups, regardless of the level-set PPMC threshold.

IV. DISCUSSION

The results in section III show that the proposed contiguity method is effective at characterising models of various spatial characteristics. However, its application to real data sets is limited by strong assumptions:

1. the paradigm stimulus has two states: "rest" and "active", which can be arbitrarily represented by 0 and 1, respectively, and

2. the imaging modality has coarse enough resolution such that the cerebrovascular capillary bed appears contiguous.

Indeed, there is no obvious rationale for modelling multi-state paradigms as a time sequence, and secondly, perhaps the true cerebral hemodynamics will not appear contiguous at a fine enough image resolution. However, most fMRI analyses may benefit from the proposed method as described.

The biophysical discovery of the paramagnetic property of deoxygenated hemoglobin led to the development of fMRI techniques for imaging cerebrovascular activity. The analysis of the acquired data is mainly based on the temporal changes of the response signal observed in each voxel. In particular, data-driven models have demonstrated the capability of clustering voxels with similar response signals.

This study proposes a novel complimentary technique for characterising the spatial distribution of such voxel maps based on a measure of contiguity. The motivations for developing a spatial analysis method is that relevant information exists in the location and distribution of the voxels, since there is a general understanding that brain function is organised in a somewhat compartmental manner. Furthermore, data-driven methods aim to identify all patterns in a data set, without *a priori* knowledge of the subject or experiment. Therefore, such analyses necessarily require a post-processing interpretation stage to determine whether any results are plausibly related to the experimental stimulus. It may be that much of this interpretation stage can be automated by robust selection criteria appealing to both temporal and spatial *priori* information.

ACKNOWLEDGEMENTS

REFERENCES

[1] W. Kuschinsky, "Regulation of cerebral blood flow," *Functional MRI* (eds. Moonen, CTW, Bandettini, PA), Germany: Springer, 2000, pp. 15-24.

[2] M. Jarmasz and R. L. Somorjai, "Exploring regions of interest with clustering analysis (EROICA)...," *Artif. Intell. Med.*, vol. 25, pp. 45-67, 2002.

[3] R. J. Adler, *The Geometry of Random Fields*, Wiley, Binghampton, NY, USA, 1981.

[4] A. Bovik, *Handbook of Image and Video Processing*, Academic Press, San Diego, CA, USA, 2000.

[5] C. Gómez-Laberge, A. Adler, I. Cameron, T. Nguyen, M. J. Hogan, "Selection criteria for the analysis of data-driven clusters in cerebral fMRI," *submitted to* IEEE Trans. Biomed. Eng., 2008.
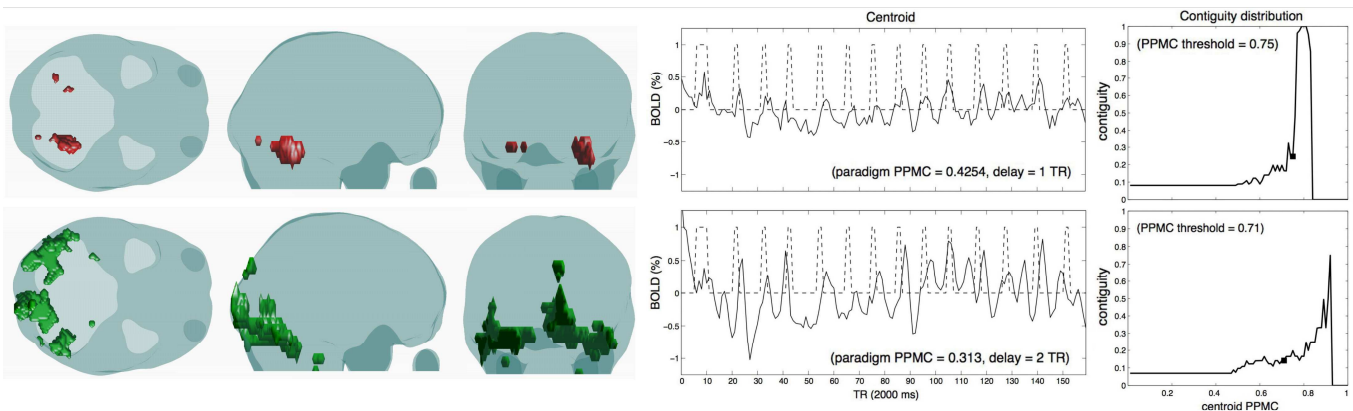

Figure 4: Cluster voxel maps resulting from fMRI BOLD data acquired during an event-related visually cued motor-task on one normal subject [5]. (*each row*) Selected cluster voxel map shown from transcranial, sagittal, and coronal views along with the anatomical outline. Centroid BOLD response (*solid*) and paradigm (*dashed*) time sequences plotted versus time in image (TR) intervals. Contiguity distribution versus voxel-centroid PPMC.